EFDA–JET–CP(13)03/23

P. Mantica, C. Angioni, M. Valisa, M. Baruzzo, P. Belo, M. Beurskens, C. Challis, E. Delabie, L. Frassinetti, C. Giroud, N. Hawkes, J. Hobirk, E. Joffrin, L. Lauro Taroni, M. Lehnen, J. Mlynar, T. Püetterich, M. Romanelli and JET EFDA contributors

Transport Analysis of Tungsten and Beryllium in JET Hybrid Plasmas with the ITER-like Wall

Transport Analysis of Tungsten and Beryllium in JET Hybrid Plasmas with the ITER-like Wall

P. Mantica[1], C. Angioni[2], M. Valisa[3], M. Baruzzo[3], P. Belo[4], M. Beurskens[5], C. Challis[5], E. Delabie[6], L. Frassinetti[7], C. Giroud[5], N. Hawkes[5], J. Hobirk[2], E. Joffrin[8], L. Lauro Taroni[3], M. Lehnen[9], J. Mlynar[10], T. Püetterich[2], M. Romanelli[5] and JET EFDA contributors*

JET-EFDA, Culham Science Centre, OX14 3DB, Abingdon, UK

1Istituto di Fisica del Plasma, CNR, Assoc. EURATOM-ENEA sulla Fusione, Milano, Italy
[2]Max Planck Institut fur Plasmaphysik, EURATOM-IPP Ass., Garching, Germany
[3]Consorzio RFX–Associazione EURATOM-ENEA sulla Fusione, Padova, Italy
[4]EURATOM/IST Fusion Ass., Instituto de Plasmas e Fusao Nuclear, Lisbon, Portugal
[5]EURATOM-CCFE Fusion Association, Culham Science Centre, OX14 3DB, Abingdon, OXON, UK
[6]EURATOM/DIFFER Association, Nieuwegein, the Netherlands
[7]Association EURATOM–VR, Fusion Plasma Physics, EES, KTH, Stockholm, Sweden
[8]Association EURATOM-CEA, CEA/DSM/IRFM, Cadarache, France
[9]Forschungszentrum Julich GmbH, EURATOM Association, Jülich, Germany
[10]EURATOM-IPP.CR Association, Institute of Plasma Physics AS CR, Prague, Czech Republic
** See annex of F. Romanelli et al, "Overview of JET Results", (24th IAEA Fusion Energy Conference, San Diego, USA (2012)).*

Preprint of Paper to be submitted for publication in Proceedings of the 40th EPS Conference on Plasma Physics, Espoo, Finland.
1st July 2013 – 5th July 2013

INTRODUCTION

The reestablishment of the hybrid scenario in JET after installation of the ITER-like wall (ILW) was successful in reaching similar global performances as in CFC wall ($H_{98} \sim 1.3$, $\beta_N \sim 3$) [1]. However, these performances have only been maintained for 2–3s, after which W accumulation in the core compromises the plasma performance, both due to radiative cooling and to the onset of MHD activity with negative effects on confinement. This paper aims at studying the dynamics of core W accumulation in hybrid plasmas, understanding its origin and possible ways to counteract it, to allow time extension of the improved confinement phase. The focus of the paper will not be on W sources from the edge, which can be regulated by e.g. gas puffing, ELMs pacing, SOL and divertor density control, which are the object of other studies [2]. The focus here will be on core impurity transport and MHD, and how they evolve during the hybrid discharge eventually leading to accumulation.

One representative low triangularity hybrid discharge (Pulse No: 82722, $B_T = 2T$, $I_p = 1.7MA$) has been selected for detailed analysis and transport simulations. The typical pattern is the time evolution of the SXR 2D emission from a bean shaped structure localized off-axis on the LFS to a very centrally peaked emission (Fig.1). The first is the outcome of a hollow W density profile in presence of strong centrifugal effects due to the high toroidal rotation [3], whilst the second is indicative of central W accumulation.

The W and Be density profiles, assumed as the two main impurities in these plasmas, have been simulated using the 1D JETTO/SANCO transport code [4]. Plasma profiles were fixed from experiment whilst impurity profiles were predicted using NCLASS [5] and empirical anomalous diffusivity and convection velocity profiles, adjusted to reproduce quantitatively SXR emission and radiation profiles, plus the Z_{eff} which is almost entirely made up by Be. The 1D JETTO/SANCO simulations can be matched to the 2D SXR data via the postprocessor UTC, which applies to the 1D simulated nW analytical expressions for the centrifugal effect of rotation such as described in [3] and then computes the 2D SXR emission, including the Bremsstrahlung component. Consistency with VUV and CX spectroscopy was also cross-checked. The spatial distribution of all ionization stages (74 for W and 4 for Be) is calculated assuming coronal equilibrium and the same anomalous transport for all ionization stages. The empirical profiles for W v/D found for Pulse No: 82722 at the two times are shown in Fig.2, where they are also compared with the first principle predictions using GKW and NEO described in [6]. The corresponding total W density profiles are shown in Fig.3. It is evident that the main difference between the two times is the presence in the region $\rho_{tor}<0.2$ (where neoclassical transport dominates) of an outward convection in the early phase, leading to very hollow W profiles, and a strong inward convection in the late phase, leading to centrally peaked W profiles. Central concentrations are $n_W/n_e \sim 1\times10^{-5}$ and $n_W/n_e \sim 1\times10^{-3}$ respectively. The key player determining so different W profiles is the density peaking in the inner plasma region, which evolves from hollow to peaked within 2–3s from the NBI switch on (Fig.4), determining the transition from outward to inward neoclassical convection. The Be concentration (~3%) and profiles

(Fig.3) obtained from best-fit process do not vary as much as the W ones between the two phases. The type of match obtained between simulated and experimental SXR line integrals is shown in Fig.5, whilst the radiation profiles are shown in Fig.6. We note that a significant contribution from Ni to SXR emission is excluded, because it would be incompatible with the measured Z_{eff} and also, with the experimental level of rotation, it would yield much less poloidal asymmetry than measured.

The pattern of W neoclassical accumulation due to progressive peaking of the central density, as described in detail for Pulse No: 82722, is common to all low triangularity hybrid pulses analysed so far, as shown in [6]. To this pattern, a variety of MHD phenomenology is often superimposed, which can also act on the W accumulation process, in opposite ways depending on the mode location with respect to the location of the W peak. A n = 1 mode is generally present in most discharges since the early phase, alternating phases of kink type with phases of tearing type often terminated by a sawtooth crash. Fig.7 shows the n = 1 mode amplitude and spectrogram in correlation with central SXR emission and central ne peaking. When W is centrally peaked, the good effect of crashes in expelling W from the centre is evident. Less obvious is to discriminate the effect of the n = 1 tearing mode. The good correlation in time between ne peaking and central SXR emission suggests that neoclassical transport remains always the driving term for accumulation. The n = 1 tearing can possibly be beneficial by flattening the n_e profile, as it seems to happen around t = 6.2s (n = 1 grows and ne peaking slowly decreases together with central SXR), whilst later it does not seem to play a role until it culminates into a crash.

Another piece of evidence in favour of the potential beneficial role of the n = 1 in counteracting W accumulation is found in the very few hybrid discharges that do not end into W accumulation (e.g. Pulse No: 83527) because they exhibit a strong n=1 central mode and a flat core ne profile. It is to be noted that the W accumulation pattern can be repeated in cycles, with central MHD crashes taking W outwards and density re-peaking after crash re-accumulating W in the centre. On the other hand, higher n NTMs appearing more off-axis can have a negative synergy with the W neoclassical accumulation when they appear in the early phase when W has a hollow profile. In such case, the effect of the island located in the same region of the W peak is that of displacing large amounts of W towards inner regions where dominant neoclassical convection will lead to accumulation. Ev idence for this phenomenology is shown in [6]. In fact, very often the initial rise of core W when ne peaks is followed by a NTM onset, which, being the W profile still hollow, further accelerates the accumulation process, as seen in Fig.8. At the same time, NTMs may contribute to dragging down the toroidal rotation, which reduces Ti peaking and further enhances the W neoclassical pinch, besides reducing core confinement.

Since the key factor underlying W accumulation is in any case the neoclassical inward convection driven by the central ne peaking, it is important to understand its origin in order to devise strategies to mitigate it thereby reducing W accumulation. To this end, the density evolution for the hybrid Pulse No: 83532 has been simulated using the first principle transport model GLF23 [7]. Figure 9 shows the time evolution of both experimental and simulated profiles. The model captures well the

transition from hollow to peaked profiles, including the timescale. It is found in simulations that a key role in the reversal of profiles from hollow to peaked is played by the NBI central particle source, consistent with the fact that the Ware pinch is very small (<0.01m/s) and the turbulent pinch is not present in this central region where turbulent transport is quenched.The low value of the central particle diffusivity enhances the effect of sources. Being $R/L_n = -Rv/D + R\Gamma_{NBI}/(D \cdot n)$, a linear correlation is expected between central NBI particle source and central R/Ln_e, if $(D \cdot n_e)$ is reasonably constant. This is shown in Fig.10. In spite of the large scatter, it is seen that ILW discharges have accessed even higher values of sources and ne peaking, likely due to concomitant upgrade of the NBI system. Such ne peaking in the presence of W is at the origin of the present problems in prolonging the improved confinement beyond 2–3s. Therefore an optimization of the choice and settings of NBI sources that would lead to reduced central particle source should be investigated. It is also expected that higher plasma currents allowing higher densities and more off-axis beam particle deposition will naturally bring to flatter central ne profile shapes favourable to avoid W accumulation. In addition, adding central ICRH power to excite core turbulence is expected to enhance both the main particle and the W diffusivities, mitigatingrespectively the density peaking and the dominance of the W neoclassical pinch. ICRH in dominant ion heating scheme may also be beneficial by increasing T_i peaking and neoclassical screening. As mentioned above, also having a strong n = 1 central mode is a way of avoiding W accumulation, although this does not appear as a promising method of control due to its negative effects also on central temperatures.

ACKNOWLEDGEMENTS

This work was supported by EURATOM and carried out within the framework of EFDA. The views and opinions expressed herein do not necessarily reflect those of the European Commission.

REFERENCES

[1]. E.Joffrin et al., Scenario development at JET with the new ITER-like wall, IAEA Fus. Energy Conf., San Diego, 2012.

[2]. T.Puetterich et al., Taming Tungsten in JET and AUG, invited talk at this conference.

[3]. J. Wesson, Nuclear Fusion **37**, 577 (1997).

[4]. L. Lauro Taroni et al., Proc. 21st EPS Conference Controlled Fusion and Plasma Physics, Montpellier, France, Vol.I, p. 102 (1994).

[5]. W. Houlberg et al., Physics of Plasmas, 4, 3231 (1997).

[6]. C.Angioni et al., Neoclassical and turbulent transport of W in toroidally rotating JET plasmas, this conference.

[7]. R.E. Waltz et al., Physics of Plasmas, **4**, 2482 (1997).

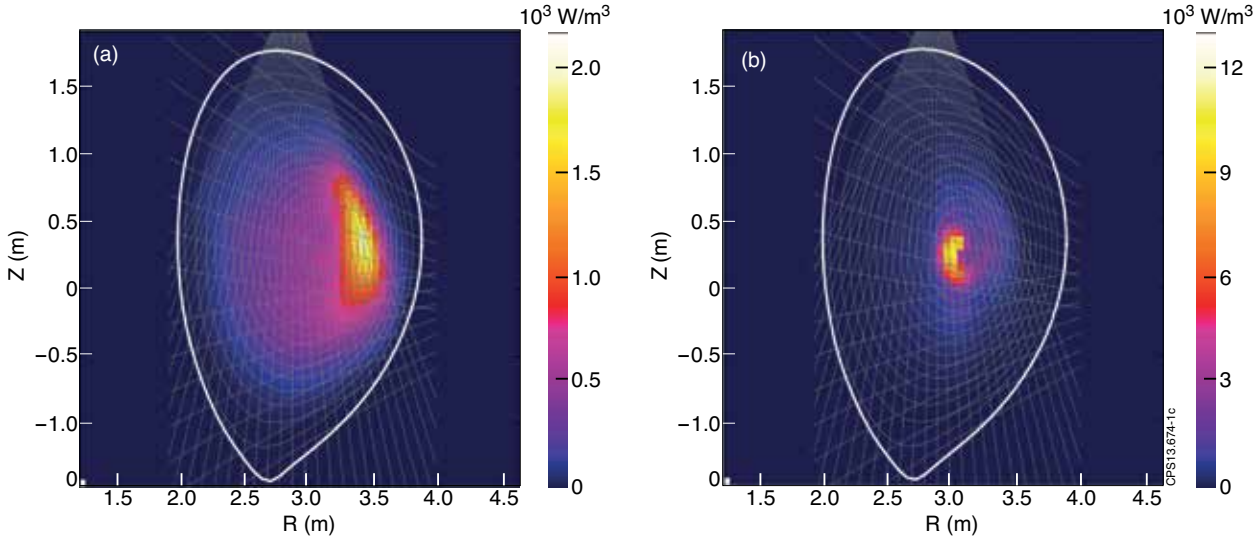

Figure 1: SXR tomography for Pulse No: 82722 a) at t = 5.9s (no W accumulation) b) at t = 7.5s (W accumulation).

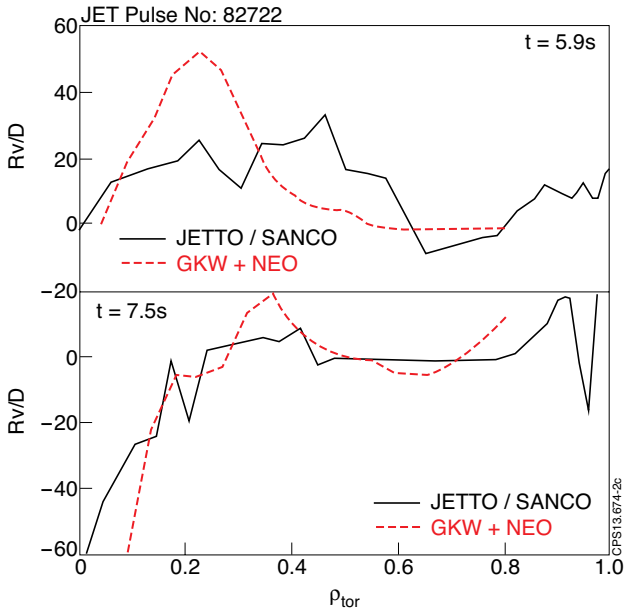

Figure 2: Profiles of W v/D obtained from bestfit of data with empirical model for Pulse No: 82722. The first principle 1D averaged v/D profiles predicted by GKW+NEO [6] are shown for comparison.

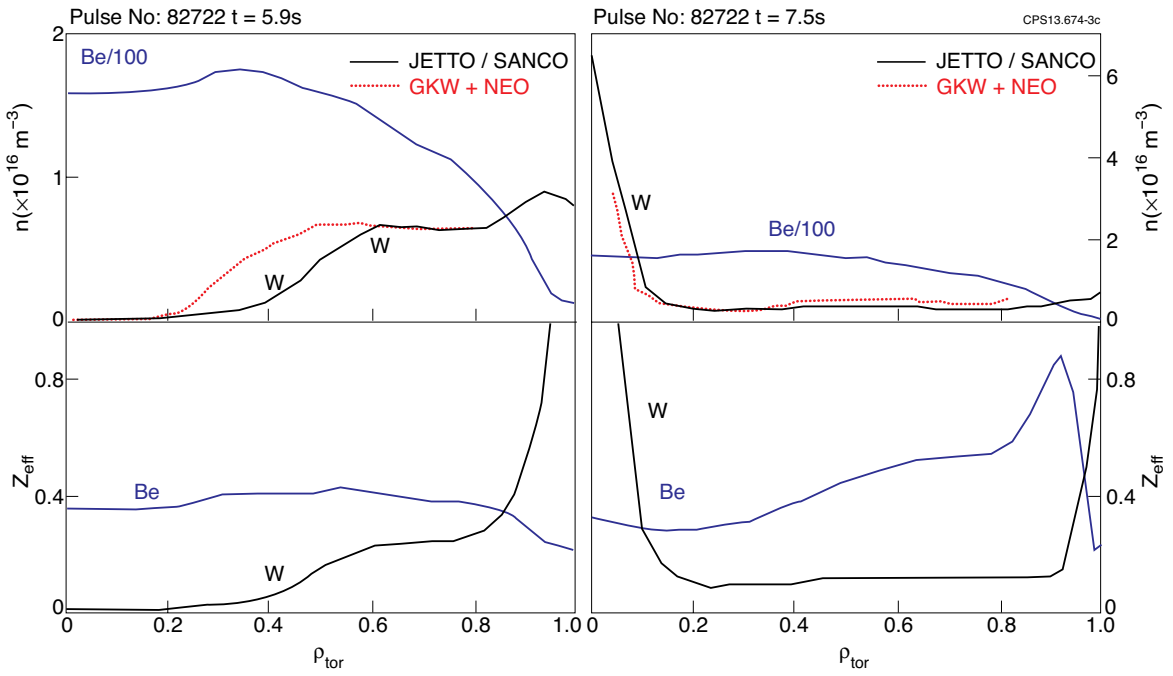

Figure 3: Top row: profiles of total density of W and Be obtained from best-fit of data using empirical transport model for Pulse No: 82722 at the two times considered. For W the GKW+NEO 1D averaged density profiles are shown for comparison. Bottom row: contribution of W and Be to Z_{eff} from JETTO/SANCO simulations.

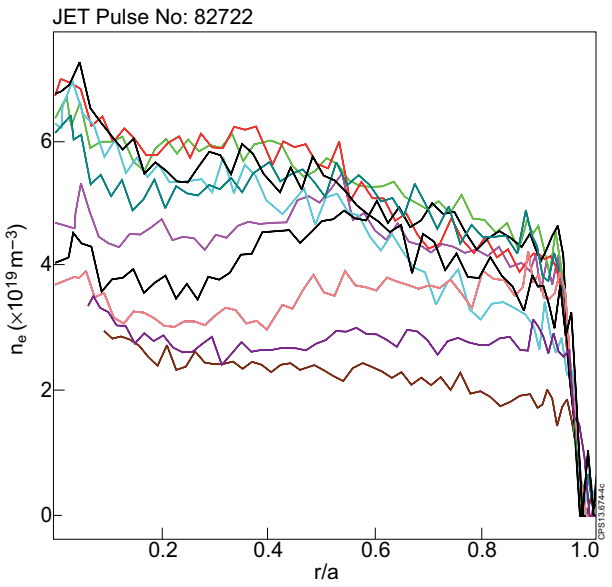

Figure 4: n_e profile evolution measured with HRTS for Pulse No: 82722

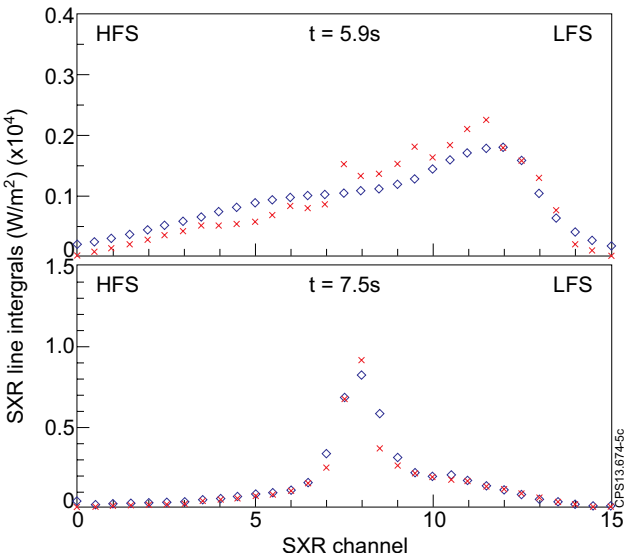

Figure 5: Comparison at two times for Pulse No: 82722 of the experimental (◊) line integrated SXR emission of the vertical camera T with the JETTO/SANCO+UTC simulated (×) SXR line integrals.

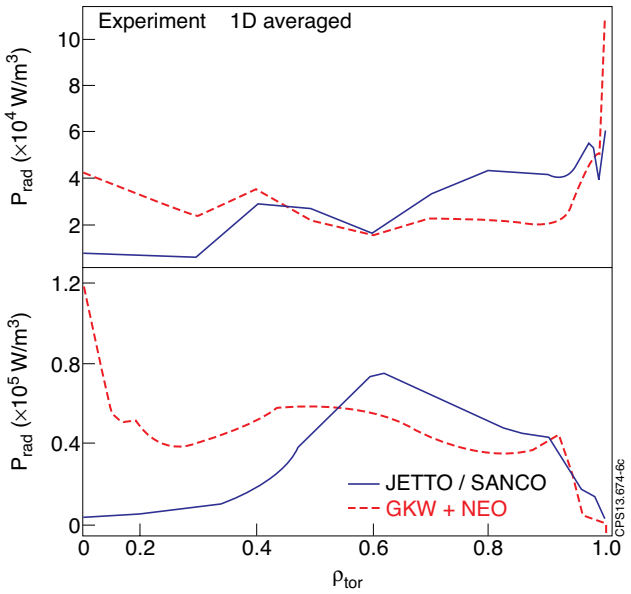

Figure 6: Comparison at two times for Pulse No: 82722 of the experimental 1D averaged radiated power density from bolometry (top) with the JETTO/SANCO simulated radiated power density (bottom).

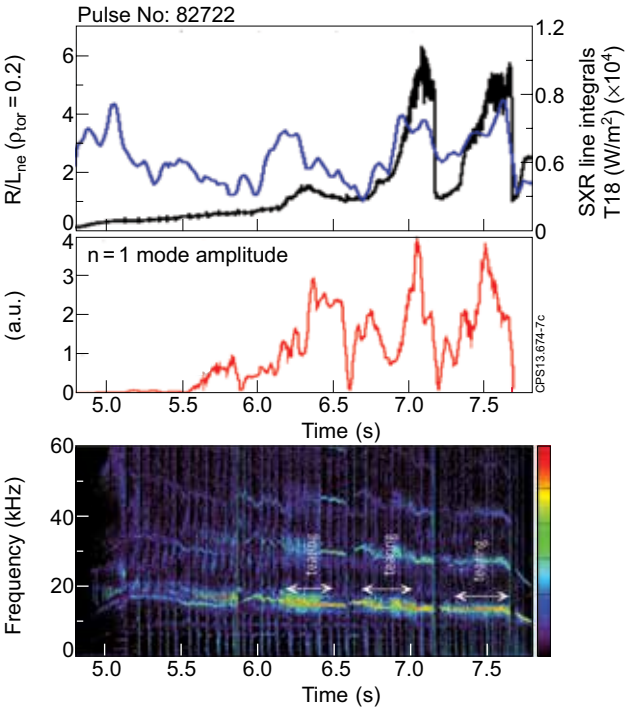

Figure 7: MHD spectrogram (c) and n=1 mode amplitude (b) for Pulse No: 82722, compared with central SXR emission (black) and central R/Ln_e (blue)(a).

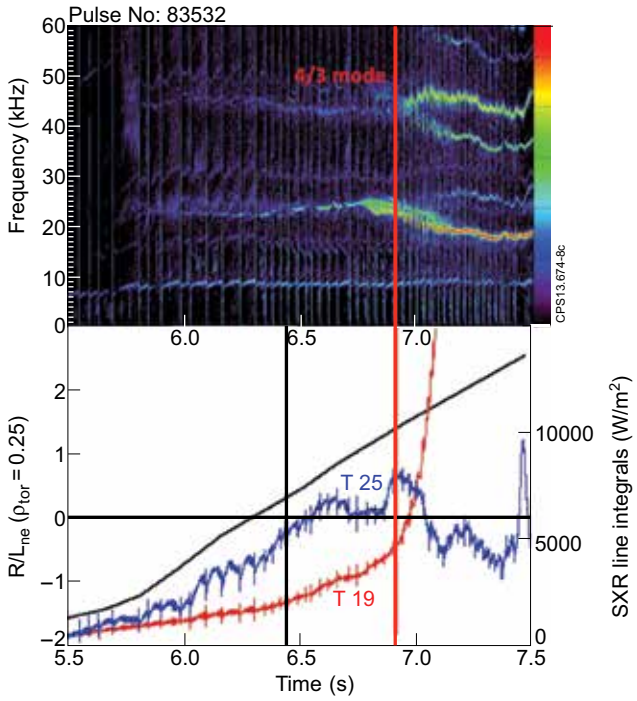

Figure 8: MHD spectrogram for Pulse No: 83532, indicating the onset of a large 4/3 NTM, correlated with the further increase of the central SXR emission (red), after the first change of rate correlated with the transition of ne profiles from hollow to peaked (R/L_{ne}>0, black line). T25 is the off-axis LFS SXR emission.

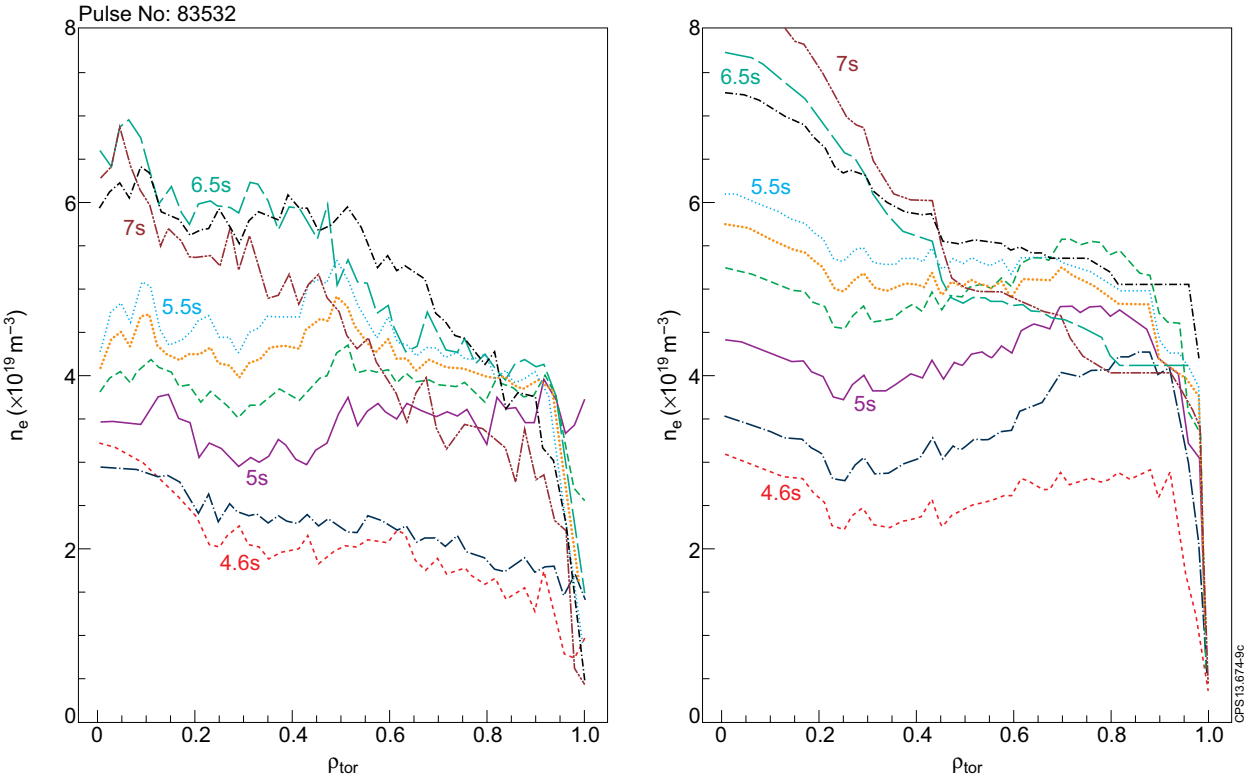

Figure 9: ne profile evolution measured with HRTS (a) and simulated using GLF23 (b) for Pulse No: 83532.

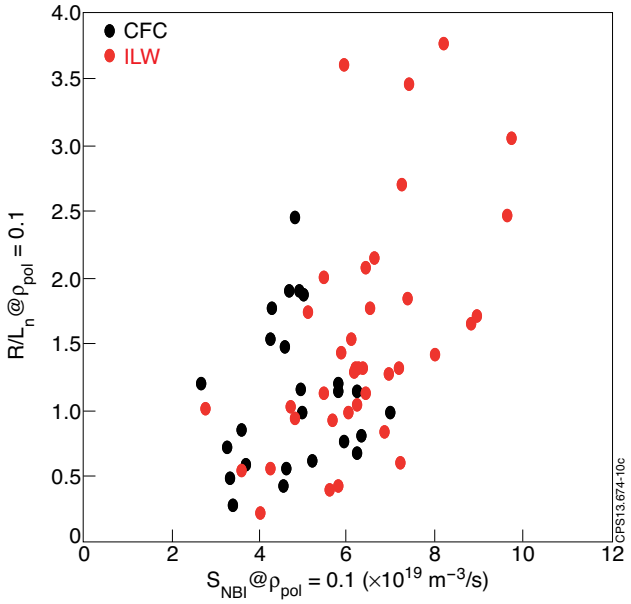

Figure 10: Correlation between R/Lne and NBI central particle source in low δ Hybrid shots with CFC (black) and ILW (red).